Thermal Spreading Resistance of Arbitrary-Shape Heat Sources on a Half-Space: A Unified Approach

Ehsan Sadeghi, Majid Bahrami, and Ned Djilali

***Abstract*—Thermal spreading/constriction resistance is an important phenomenon where a heat source/sink is in contact with a body. Thermal spreading resistance associated with heat transfer through the mechanical contact of two bodies occurs in a wide range of applications. The real contact area forms typically a few percent of the nominal contact area. In practice, due to random nature of contacting surfaces, the actual shape of microcontacts is unknown; therefore, it is advantageous to have a model applicable to any arbitrary-shape heat source. Starting from a half-space representation of the heat transfer problem, a compact model is proposed based on the generalization of the analytical solution of the spreading resistance of an elliptical source on a half-space. Using a "bottom-up" approach, unified relations are found that allow accurate calculation of spreading resistance over a wide variety of heat source shapes under both isoflux and isothermal conditions.**

***Index Terms*—Elliptical heat source, half-space, spreading resistance, square root of area, superposition.**

NOMENCLATURE

A	Area (m^2).
a	Major semi-axis (m).
$B(\cdot,\cdot)$	Beta function.
b	Minor semi-axis (m).
$K(\cdot)$	Complete elliptic integral of the first kind (7).
k	Thermal conductivity (W/m $\cdot$ K).
$\mathcal{L}$	Characteristic length scale (m).
N	Number of sides of a regular polygon.
n	Geometric parameter for hyperellipse.
Q	Heat flow rate (W).
q	Heat flux ($\mathrm{W/m}^2$).
R	Thermal spreading resistance (K/W).
$\overline{R}$	Average temperature based thermal spreading resistance (K/W).
R_0	Centroidal temperature based thermal spreading resistance (K/W).
R^*	Nondimensional spreading resistance.
R_T	Thermal spreading resistance, isothermal source (K/W).
r	Radius (m).
$\overline{T}$	Average temperature (K).
T_0	Centroidal temperature (K).

Greek Letters

α	Angle (rad).
β	Length ratio, b/a.
$\Gamma(\cdot)$	Gamma function.
ϵ	Aspect ratio.
η	Length, x_c/r.
ρ	Distance in polar coordinate (m).
ω	Angle (rad).

Subscript

c	Geometrical center of area.

Manuscript received March 13, 2008; revised November 7, 2008 and September 24, 2009. Date of current version June 9, 2010. This work was financially supported by the Natural Sciences and Engineering Research Council (NSERC) of Canada, discovery grant. Recommended for publication by Associate Editor K. Ramakrishna upon evaluation of reviewers' comments.

E. Sadeghi and N. Djilali are with the Department of Mechanical Engineering, University of Victoria, Victoria, BC V8W 2Y2, Canada (e-mail: ehsans@uvic.ca; ndjilali@me.uvic.ca).

M. Bahrami is with the School of Engineering, Simon Fraser University, Burnaby, BC V5A 1S6, Canada (e-mail: mbahrami@sfu.ca).

Digital Object Identifier 10.1109/TCAPT.2010.2043843

I. INTRODUCTION

SPREADING resistance, also sometimes referred to as constriction resistance, is commonly encountered in thermal engineering whenever a concentrated heat source is in contact with a larger heat conducting surface. This phenomenon extends also to electric current and mass transfer problems. In this paper, we focus on thermal spreading resistance which often appears as a bottleneck in heat management, and is of relevance in applications such as integrated circuits and laser heating. In contacting bodies, real interaction between two surfaces occur only over microscopic contacts [1], [2]. The actual area of contact, i.e., the total area of all microcontacts, is typically less than 2% of the nominal contact area [1], [2]. Thus, heat flow is constricted and then spreads to pass from the contact area to contacting bodies. Thermal spreading resistance plays a vital role in the design of numerous thermal, electrical, and electronic devices and systems. Electronic equipment, aircraft structural joints, surface thermocouples, boundary lubrication, nuclear reactors, biomedical industries, and cryogenic liquid storage devices are only a few examples of such systems [3]–[7].

Assuming dimensions of microcontacts and/or heat sources are small compared with the distance separating them and with the dimensions of the body which heat spreads through, the heat source on a half-space hypothesis can be used [8]. As the microcontacts or heat sources increase in number and grow in size, a flux tube problem should be considered to account

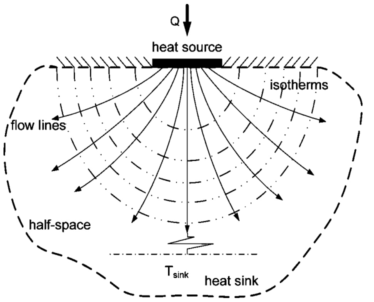

Fig. 1. Arbitrary-shape heat source on a half-space.

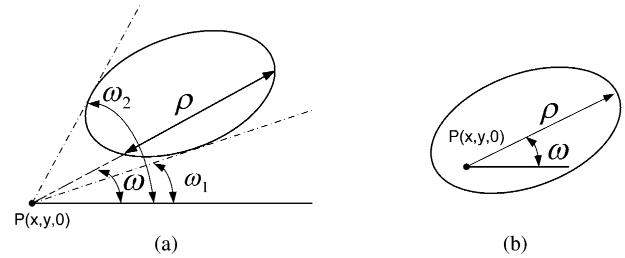

Fig. 2. (a) Point outside the heat source. (b) Point inside the heat source.

for the interference between neighboring microcontacts/heat sources. For an in-depth review of flux tube solutions for spreading resistance see [4], [9]–[11].

Several researchers including Kennedy [6], Ellison [12], Karmalkar *et al.* [13], and Pawlik [14] focused on analyzing thermal spreading resistance in electronic devices.

Yovanovich and his coworkers [15]–[18] investigated a range of steady-state and transient thermal spreading resistance. They proposed thermomechanical models for contact, gap, and joint resistances of joints formed by conforming rough surfaces, nonconforming smooth surfaces, and nonconforming rough surfaces [7]. Applying superposition techniques, Yovanovich developed a method to evaluate spreading resistance of different shapes on a half-space and derived found relationships for geometries including singly and doubly connected heat sources such as: hyperellipse, semicircle, triangle, polygon, and annulus. They also introduced the use of the square root of the source area $\sqrt{A}$ to nondimensionalize spreading resistance.

Analytical, experimental, and numerical models have been developed to predict thermal spreading resistance since the 1930s. Several hundred papers on thermal spreading resistance have been published which illustrates the importance of this topic.

In practice, due to the random nature of contacting surfaces, the actual shape of microcontacts is unknown; therefore, it would be beneficial to have a model applicable to any arbitrary-shape heat source. In spite of the rich body of literature on spreading resistance, there is yet no general model which can accurately estimate the spreading resistance of an arbitrary-shape heat source on a half-space due to the challenge of dealing with complex irregular geometries.

In this paper, a compact model is proposed based on the analytical solution of the spreading resistance of an elliptical source on a half-space. Using a "bottom-up" approach, it is shown that for a broad variety of heat source shapes, the proposed model is in agreement with the existing and/or developed analytical solutions.

II. Problem Statement

Consider steady-state heat transfer from an arbitrary-shape planar singly connected heat source on a half-space, Fig. 1. The temperature field within the half-space must satisfy Laplace's equation, $\nabla^2 T = 0$.

Thermal spreading resistance R is defined as the difference between the temperature of heat source and the temperature of a heat sink far from it divided by the total heat flow rate through the contact area Q; i.e., $R = \Delta T/Q$ [19]. For convenience, the temperature far from the contact area may be assumed to be zero with no loss of generality, that is

$$R = \frac{T}{Q}. \tag{1}$$

To evaluate the spreading resistance, the temperature distribution of the heat source is required. Yovanovich [15] developed a relationship for the temperature distribution at each point of an isoflux heat source plane by using the integral and superposition techniques

$$T(x, y, 0) = \frac{q}{2\pi k} \int_0^{\omega} \rho(\omega) d\omega \tag{2}$$

where ρ and ω are shown in Fig. 2 for points outside and inside of the heat source area.

The reference temperature of heat sources is usually considered as the centroid or the average temperature. Substituting geometric center coordinates into (2), the centroid temperature can be found. For the average temperature, the temperature distribution is integrated over the heat source area

$$\overline{T} = \frac{1}{A} \int\int_A T(x, y, 0)\, dA. \tag{3}$$

For complicated shapes, the geometry is subdivided into simpler shapes; $T(x, y, 0)$ is then computed from (2) for each subdivided shape and the values are added up. Once the temperature is determined, the spreading resistance is obtained through (1).

To investigate the trend of different shapes and aspect ratios, it is more convenient to nondimensionalize spreading resistance in the form of $R^* = k\ \mathcal{L}\ R$, where k, $\mathcal{L}$, and R are the thermal conductivity of half-space, a characteristic length scale, and the spreading resistance, respectively [16]. Parameters required to define spreading resistance are: reference temperature, characteristic length scale, and boundary condition, (see Fig. 3). The reference temperature can be the centroid or average temperature of the source. According to Yovanovich [16], spreading resistance values for hyperelliptical sources vary over narrower bond when based on the centroidal temperature rather than when based on the average temperature. As shown later, there is a relationship

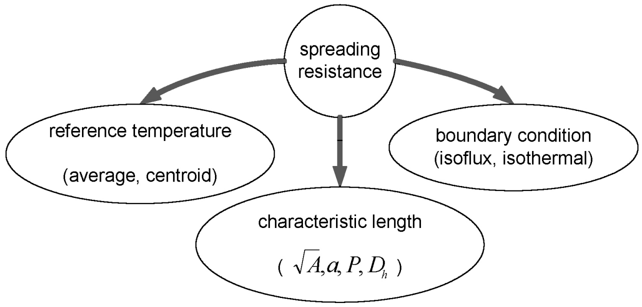

Fig. 3. Parameters involved in spreading resistance solution.

between the average and the centroid based resistances; for convenience, the average temperature is used as the reference temperature. After examining several possible length scales, we concluded that the square root of the square area $\sqrt{A}$ is the best choice of characteristic length scale, as Yovanovich proposed [16]. The next parameter is boundary condition; two boundary conditions are considered: 1) isothermal and 2) isoflux. The isoflux boundary condition is easier to apply and solve for. Furthermore, a relationship between these boundary conditions can be established.

III. Characteristic Length Scale

To nondimensionalize the spreading resistance, a characteristic length scale is required. Different characteristic length scales are examined in this section. These include perimeter P, hydraulic diameter ($D_h = 4A/P$), an arbitrarily chosen dimension a, and the square root of the source area $\sqrt{A}$.

An analytical solution exists for hyperellipse shapes in the literature [16]. To compare different characteristic length scales, a hyperellipse source covering a wide variety of geometries is selected. A hyperellipse, in the first quadrant, is described by

$$y = b\left[1 - \left(\frac{x}{a}\right)^n\right]^{1/n} \tag{4}$$

where a and b are characteristic dimensions along the x and y axes, respectively, see Fig. 4. The effect of parameter n on the shape of the hyperellipse source is also shown in Fig. 4. When $n = 1$, the hyperellipse yields a rhombic source ($a > b$), or a square ($a = b$); for $n = 2$, the source is elliptical ($a > b$), or circular ($a = b$); $n > 3$, yields a rectangle ($a > b$) or a square ($a = b$) source with rounded corners; and for $n \to \infty$, the shape approaches a full rectangle/square source [16].

Yovanovich [16] calculated the spreading resistance for hyperelliptical sources. For instance, the nondimensional spreading resistance with $\sqrt{A}$ as the characteristic length scale is [16]

$$k\sqrt{A}R_0 = \frac{1}{\pi}\sqrt{\frac{\epsilon n}{B\left(\dfrac{n+1}{n}, \dfrac{1}{n}\right)}}\int_0^{\pi/2} \frac{d\omega}{[\sin^n \omega + \epsilon^n \cos^n \omega]^{1/n}} \tag{5}$$

where $B(\cdot)$ is the beta function.

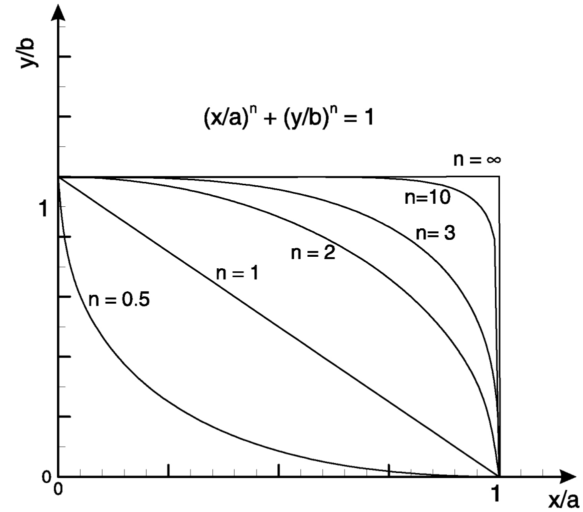

Fig. 4. Hyperellipse heat source in the first quadrant.

The analytic nondimensional spreading resistances R^* obtained using four different characteristic length scales are compared in Fig. 5(a)–(d) for both rectangular and elliptical sources. Comparing the trends for the different characteristic length scales, it can be concluded that the square root of area $\sqrt{A}$ is the superior choice for characteristic length scale. With this choice, the maximum difference between the analytical solutions of elliptical and rectangular sources is less than 6.8%; and in fact for $\epsilon > 0.4$, the difference is less than 1.5%. Since elliptical and rectangular sources, corresponding to (4) with $n = 2$ and $n \to \infty$, cover a wide range of shapes, it can be concluded that using $\sqrt{A}$ as a characteristic length scale, nondimensional spreading resistance of a hyperellipse with any value of $2 < n < \infty$ differ less than 6.8% with respect to an elliptical source. This implies that the effect of corners on the spreading resistance is not significant for hyperelliptical shapes with identical areas and aspect ratios. Since a hyperellipse covers a wide variety of shapes, the square root of area $\sqrt{A}$ is the most appropriate characteristic length scale for any arbitrary-shape heat source on a half-space, as Yovanovich suggested [16].

IV. Proposed Model

As shown previously, nondimensional spreading resistances of hyperelliptical sources with equal areas and aspect ratios are close for any value of $2 \le n \le \infty$. Thus, if we select one of these shapes in the model, the spreading resistance of the others can be predicted with good accuracy. The premise of the present model is that the solution for hyperelliptical source can be applied to estimate the spreading resistance of any shape of heat sources when the area and aspect ratio are the same as those of the hyperelliptical source. Since, the analytical solution of the elliptical source is more convenient, it is chosen as the basis of the model. Note that the isoflux rectangle could also be used as the basic model, but subsequent analysis has shown that the isoflux ellipse provides better overall agreement. According to the present model, an arbitrary-shape heat source is transformed to an elliptical shape where area and aspect ratio are maintained constant, (see Fig. 6). The

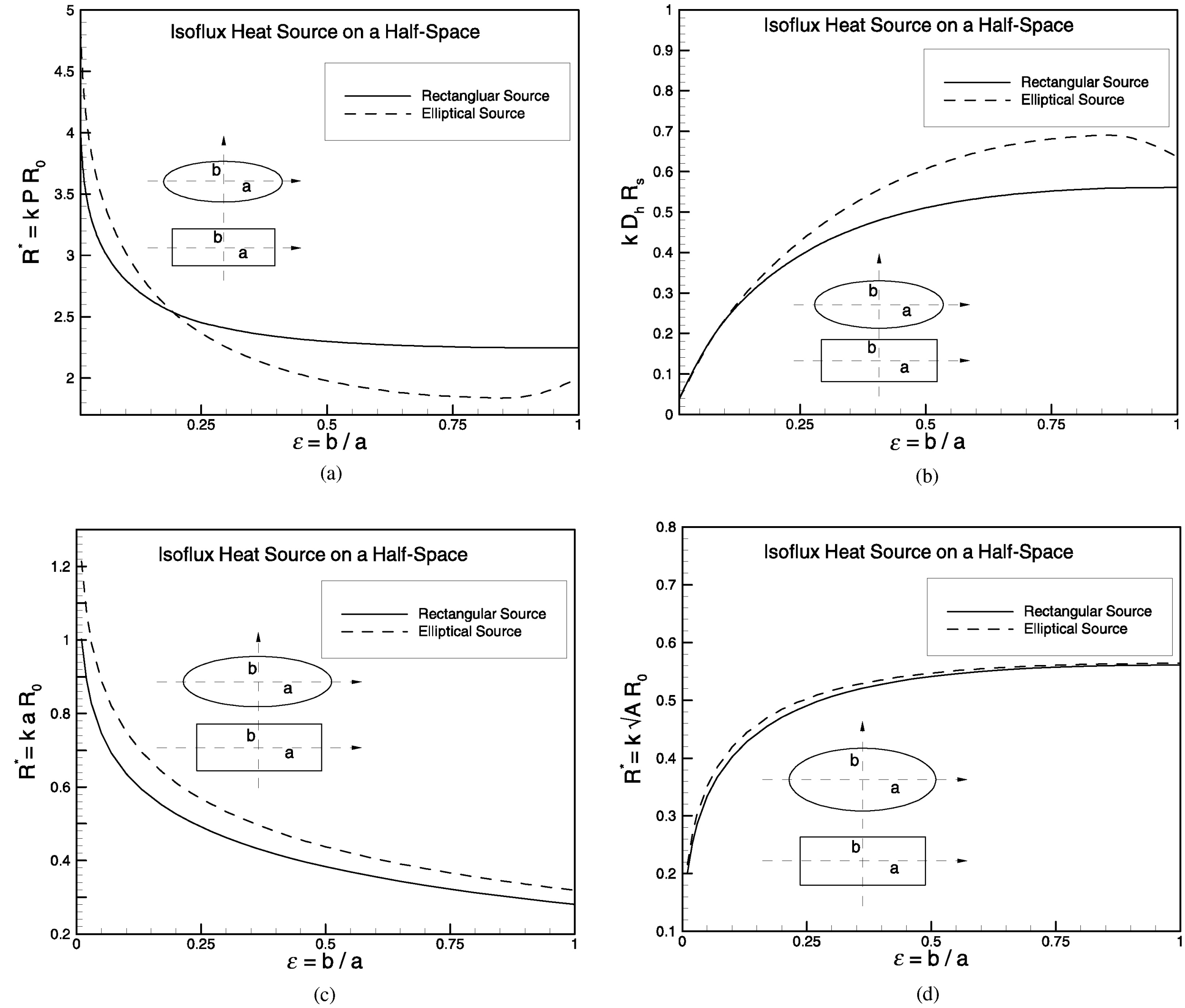

Fig. 5. Nondimensional spreading resistance of rectangular and elliptical sources with the characteristic lengths. (a) Perimeter P. (b) Hydraulic diameter D_h; (c) Major semi-axes a. (d) Square root of area $\sqrt{A}$.

analytical solution for the spreading resistance of an isoflux elliptical source on a half-space can be expressed using the general solution proposed by Yovanovich for a hyperellipse [15]

$$k\sqrt{A}R_0 = \frac{2}{\pi\sqrt{\pi}} \frac{K(1-\frac{1}{\epsilon^2})}{\sqrt{\epsilon}} \tag{6}$$

where $K(\cdot)$ is the complete elliptic integral of the first kind defined as

$$K\left(1-\frac{1}{\epsilon^2}\right) = \int_0^{\pi/2} \frac{dt}{\sqrt{\left[1-\left(1-\frac{1}{\epsilon^2}\right)\sin^2 t\right]}}. \tag{7}$$

There are a number of possible ways of defining the aspect ratio for arbitrary shapes, and in this paper the following is adopted

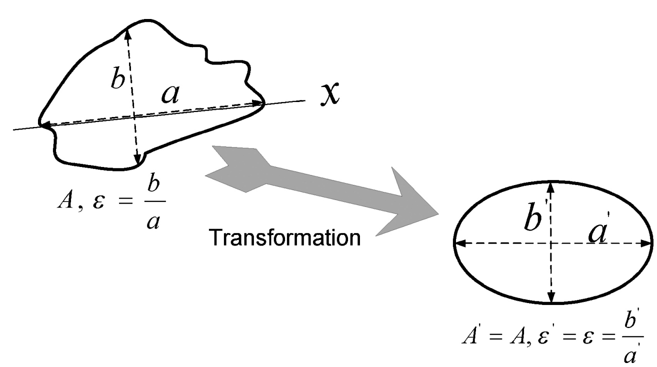

Fig. 6. Geometrical transformation of any arbitrary-shape heat source to elliptical source.

$$\epsilon = \frac{b}{a} \tag{8}$$

where a is the maximum length of the shape in arbitrary direction of x and b is the maximum length in the perpendicular

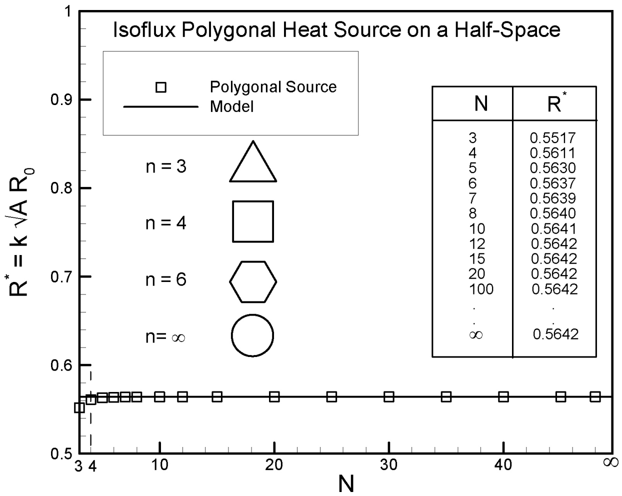

Fig. 7. Comparison of polygonal heat source with the model.

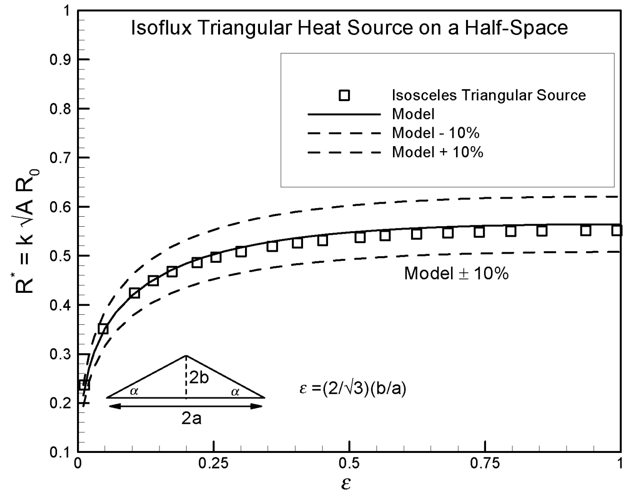

Fig. 8. Comparison of isosceles triangular heat source with the model.

direction to x as shown in Fig. 6. This definition, though not necessarily general, is appropriate for most of the shapes considered in this paper.

V. Comparison With Analytical Solutions

Using the superposition and integral methods proposed by Yovanovich [15], we find analytical solutions for spreading resistance of trapezoidal, rhombic, circular sector, circular segment, and rectangular source with semicircular or round ends as reported in the proceeding sections. In this section, the proposed model is compared with available and developed analytical solutions for a wide variety of isoflux heat sources on a half-space.

A. Polygonal Source

The analytical solution for a regular polygonal source with N sides can be written as [15]

$$k\sqrt{A}R_0 = \frac{1}{\pi}\sqrt{\frac{N}{\tan(\pi/N)}}\ln\frac{1+\sin(\pi/N)}{\cos(\pi/N)}. \tag{9}$$

Fig. 7 shows the effect of number of sides N on the nondimensional spreading resistance. There is not much difference between the different polygons, and for $N \geq 6$ the results are essentially the same. Also, the results are compared with the model for $\epsilon = 1$; the maximum difference between the analytical solution of polygonal sources and the model is less than 2.2%.

B. Triangular Source

The analytical solution for an isosceles triangular isoflux source developed by Yovanovich [15] is given by

$$k\sqrt{A}R_0 = \frac{\sqrt{2\beta}}{3\pi}\left[\ln\left[\tan\left(\frac{\pi}{4}+\frac{\omega_1}{2}\right)\right] + 2\sin(\cot^{-1}2\beta)\times \ln\left[\tan\left(\frac{\pi}{4}+\frac{\omega_2}{2}\right)\tan\left(\frac{\pi}{4}+\frac{\omega_3}{2}\right)\right]\right] \tag{10}$$

where $\omega_1 = \tan^{-1}(3/2\beta)$, $\omega_2 = \pi/2 - \cot^{-1}(2\beta)$, $\omega_3 = \pi - \omega_1 - \omega_2$, and $\beta = b/a$.

Choosing a proper aspect ratio is important. The aspect ratio for an equilateral triangle is unity; hence, the aspect ratio that also satisfies the equilateral case is $\epsilon = \beta(2/\sqrt{3})$. The spreading resistance for isosceles triangular source is compared with the model in Fig. 8. Results show good agreement with the model and maximum error is less than 2.2% when $\epsilon > 0.1$.

C. Rhombic Source

A rhombus is a special case of hyperellipse with $n = 1$. The spreading resistance for this shape can be evaluated from (5). A simpler method to calculate it, would be using the superposition technique. The nondimensional spreading resistance for a rhombic source can be written as

$$k\sqrt{A}R_0 = \frac{\sqrt{2}\sin(\omega_1)}{\pi\sqrt{\epsilon}}\ln[\tan(\frac{\pi}{4}+\frac{\omega_1}{2})\tan(\frac{\pi}{4}+\frac{\omega_2}{2})] \tag{11}$$

where $\omega_1 = \tan^{-1}\epsilon$, $\omega_2 = \pi/2 - \omega_1$, $A = 2ab$, and $\epsilon = b/a$.

Fig. 9 compares the rhombic heat source solution and the model, (6); except for small value of aspect ratio, $0 < \epsilon < 0.25$, the results agree with the model within 1.7%. The agreement for the lower aspect ratios is within 10%.

D. Trapezoidal Source

The trapezoidal cross-section is an important geometry which in the limit when the top side length goes to zero, yields an isosceles triangle. At the other limit when top and bottom sides are equal, it becomes a rectangle/square.

The spreading resistance for a trapezoidal source is found using superposition technique. The relationship for a trapezoidal source is unwieldy, and is therefore given in the appendix. The comparison of the results with the model for various trapezoidal sources is shown in Fig. 10; again there is good overall agreement with the model and the difference is less than 4% when $\epsilon > 0.1$.

E. Rectangular Source With Round Ends

Rectangular heat source with round ends is a combination of triangular and circular sector sources. Using superposition

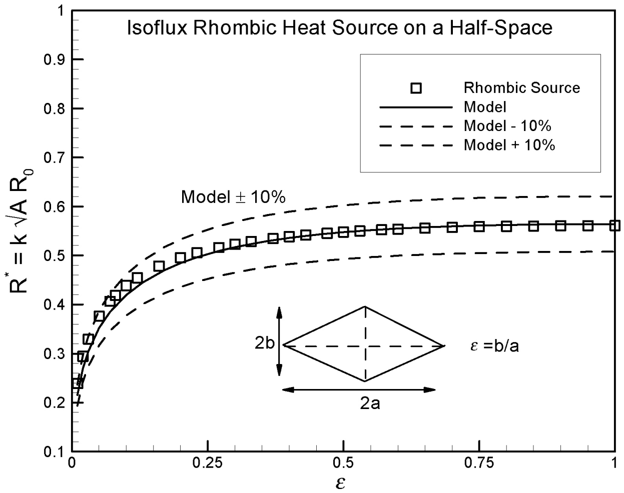

Fig. 9. Comparison of rhombic heat source with the model.

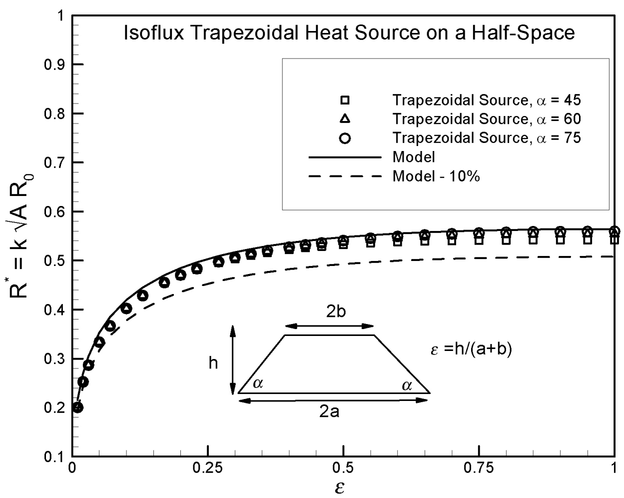

Fig. 10. Comparison of different trapezoidal heat sources with the model.

technique, the exact solution for this source is

$$k\sqrt{A}R_0=\frac{\sqrt{2}}{\pi}\frac{\beta\ln\left[\tan\left(\frac{\pi}{4}+\frac{\omega_1}{2}\right)\right]+\sqrt{1+\beta^2}\tan^{-1}\beta}{\sqrt{(1+\beta^2)\tan^{-1}\beta+\beta}} \tag{12}$$

where $\omega_1 = (\pi/2) - \tan^{-1}\beta$, $A = 2a^2[(1+\beta^2)\tan^{-1}\beta + \beta]$, $\beta = b/a$, and $\epsilon = \beta/\sqrt{1+\beta^2}$.

Fig. 11 shows the analytical solution compared with the model. It can be seen that the model can estimate the spreading resistance of this shapes with the maximum error of 2% where $\epsilon > 0.2$.

F. Rectangular Source With Semicircular Ends

Rectangular heat source with semicircular ends is a combination of triangular and circular segment sources. Using superposition technique, the exact solution for this source is

$$k\sqrt{A}R_0 = \frac{2}{\pi\sqrt{4\beta+\pi\beta^2}} \times \left[\beta\ln\left[\frac{\pi}{4}+\frac{\omega_1}{2}\right] + \int_0^{\alpha}\left(\cos\omega + \sqrt{\beta^2-\sin^2\omega}\right)d\omega\right] \tag{13}$$

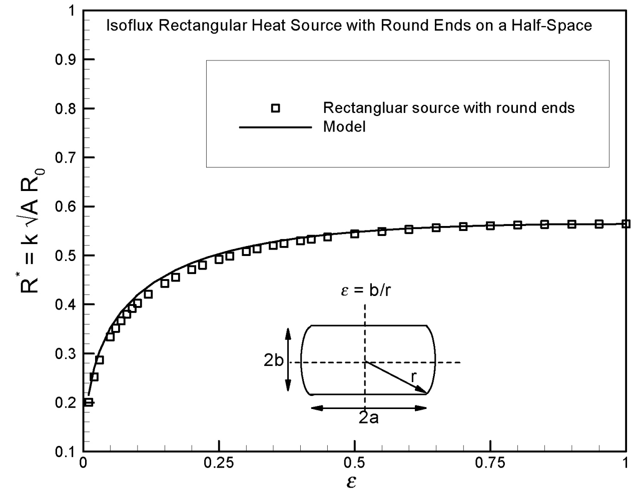

Fig. 11. Comparison of "rectangular heat source with round ends" with the model.

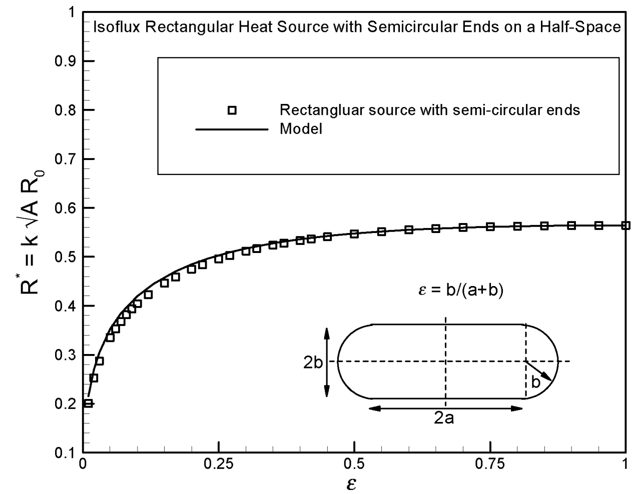

Fig. 12. Comparison of "rectangular heat source with semicircular ends" with the model.

where $\alpha = \tan^{-1}\beta$, $\omega_1 = (\pi/2) - \alpha$, $\beta = b/a$, $A = a^2[4\beta + \pi\beta^2]$, and $\epsilon = \beta/(1+\beta)$. Fig. 12 shows that the model can predict the spreading resistance for this shape with the maximum error of 2% where $\epsilon > 0.27$.

G. Circular Sector Source

Circular sector is composed of triangular and noncircular sector sources with the common vertex at the centroid. Using superposition, the exact solution can be written as

$$k\sqrt{A}R_0 = \frac{1}{\pi\sqrt{\alpha}}\left[\eta\sin\alpha\ln\left[\tan\left(\frac{\pi}{4}+\frac{\omega_1}{2}\right)\tan\left(\frac{\pi}{4}+\frac{\omega_2}{2}\right)\right] + \int_0^{\omega_3}\left(\sqrt{1-\eta^2\sin^2\omega} - \eta\cos\omega\right)d\omega\right] \tag{14}$$

where $\eta = x_c/r = 2\sin\alpha/3\alpha$, $\omega_1 = \pi/2 - \alpha$, $\omega_2 = \tan^{-1}\left[(1-\eta\cos\alpha)/(\eta\sin\alpha)\right]$, $\omega_3 = \pi - \omega_1 - \omega_2$. The aspect ratio is defined as the ratio of maximum lengths in y and x directions, i.e., $\epsilon = 2r\sin\alpha/r = 2\sin\alpha$.

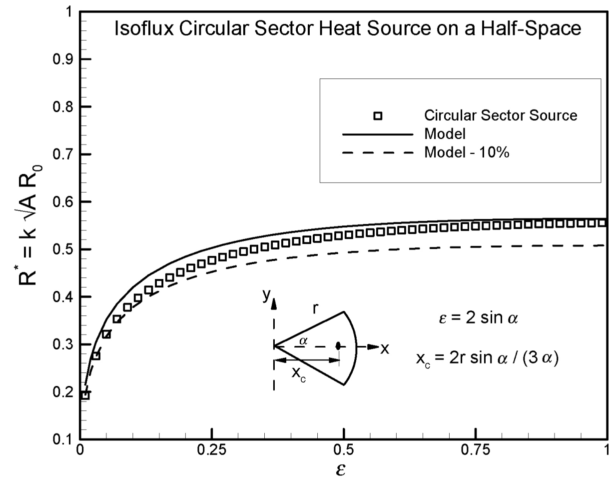

Fig. 13. Comparison of circular sector heat source with the model.

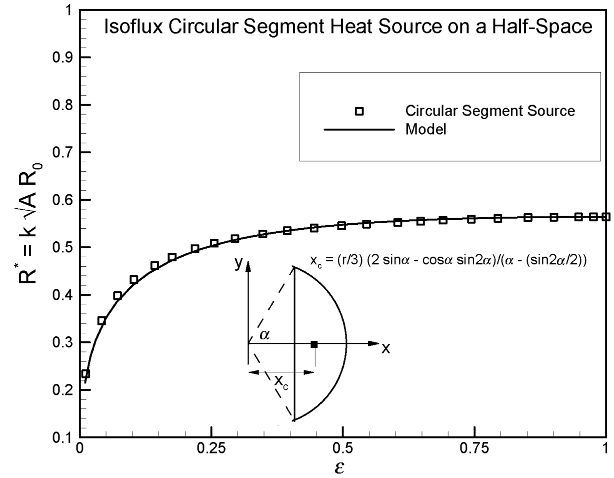

Fig. 14. Comparison of circular segment heat source with the model.

The relationship developed for the circular sector source is compared with the model in Fig. 13. Note that since η and ω_1 are functions of α only, and since $\alpha = \sin^{-1}(\epsilon/2)$, (14) can be plotted as a function of ϵ only. It can be observed that for small values of aspect ratios, the error is more than 5%, but for $\epsilon > 0.27$ the error becomes less than 5%.

H. Circular Segment Source

A circular segment can be presented as a combination of right angle triangles and noncircular sector sources with the common vertex at the geometric center. Applying (2) and using superposition technique, the exact solution for the spreading resistance can be found

$$k\sqrt{A}R_0 = \frac{1}{\pi\sqrt{\alpha - \dfrac{\sin 2\alpha}{2}}}\left[(\eta - \cos\alpha)\ln\left[\tan\left(\frac{\pi}{4} + \frac{\omega_1}{2}\right)\right] + \int_0^{\omega_2}\left(\sqrt{1 - \eta^2 \sin^2\omega} - \eta\cos\omega\right)d\omega\right] \quad (15)$$

where $x_c = \dfrac{(r/3)(2\sin\alpha - \cos\alpha \sin 2\alpha}{\alpha - \sin(2\alpha)/2}$, $\eta = x_c/r$, $\omega_1 = \tan^{-1}\left[\sin\alpha/(\eta - \cos\alpha)\right]$, and $\omega_2 = \pi - \omega_1$. The aspect ratio is defined as the ratio of maximum lengths in y and x directions. For different value of α, the aspect ratio becomes

$$\epsilon = \begin{cases} \dfrac{1 - \cos\alpha}{2\sin\alpha}, & \alpha \le \dfrac{\pi}{2} \\ \dfrac{1 - \cos\alpha}{2}, & \dfrac{\pi}{2} \le \alpha \le \pi. \end{cases} \quad (16)$$

The exact solution of the circular segment source is compared with the model in Fig. 14. The results show good agreements with the model over the entire range of aspect ratio.

The examined geometries of a heat source on a half-space are compared with the model in Table I and Fig. 15. The definition of aspect ratio, proper criteria to use the model, and the maximum relative error with respect to the model is reported in Table I. The maximum error occurs in small values of aspect ratio, $\epsilon \le 0.01$; if aspect ratio is greater than 0.1 the error decreases sharply. As seen in Table I and Fig. 15, the model shows good agreement with the analytical solutions for wide variety of shapes, especially when $\epsilon > 0.1$.

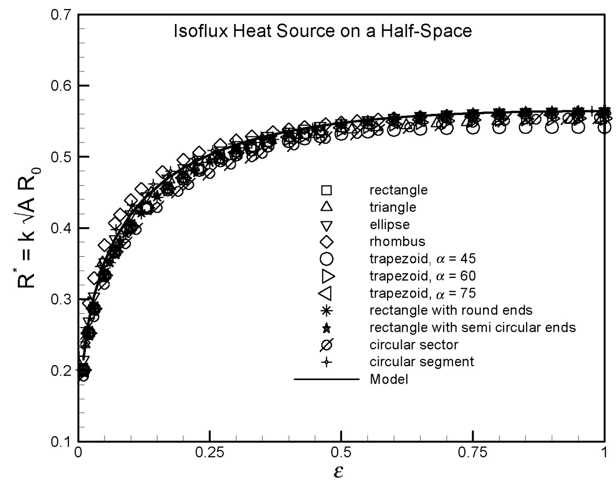

Fig. 15. Comparison of arbitrary-shape heat sources with the model.

VI. Reference Temperature

Having established the accuracy of the proposed model provides for the centroidal temperature based spreading resistance of any arbitrary-shape isoflux heat source on a half-space, we turn our attention to developing a relationship between the centroid temperature and average temperature based spreading resistances. The latter is a commonly used reference and can also be applied to doubly-connected regions.

There is no analytical solution for the isothermal elliptical source in the literature, therefore, this problem was solved numerically in this paper. The results show that the ratio of nondimensional spreading resistances based on the average and centroid temperatures for elliptical source varies only

TABLE I
COMPARISON AND ACCURACY OF PROPOSED SPREADING RESISTANCE MODEL FOR VARIOUS GEOMETRIES

cross-section	ϵ	notes	max error
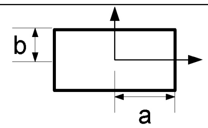	$\frac{b}{a}$	maximum difference of 2% for $\epsilon > 0.3$	6.8%
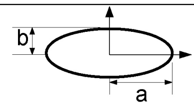	$\frac{b}{a}$	base model	–
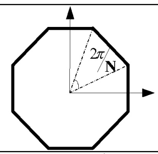	1	very close agreement with the model specially for $N > 6$	2.2%
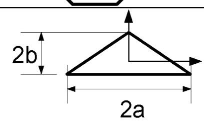	$\frac{2\beta^{[1]}}{\sqrt{3}}$	maximum difference of 2.2% for $\epsilon > 0.1$	4.8%
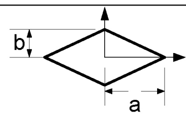	$\frac{b}{a}$	maximum difference of 1.7% for $\epsilon > 0.25$	11%
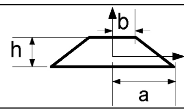	$\frac{h}{a+b}$	2.6% $<$ difference $<$ 4% for $\epsilon > 0.1$	6.8%
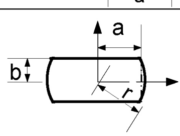	$\frac{\beta}{\sqrt{1+\beta^2}}$	maximum difference of 2% for $\epsilon > 0.2$	6.8%
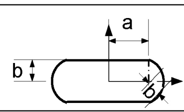	$\frac{\beta}{1+\beta}$	maximum difference of 2% for $\epsilon > 0.27$	6.8%
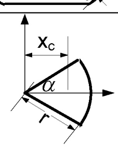	$2\sin\alpha$	maximum difference of 5% $\epsilon > 0.27$	10.8%
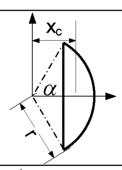	$\frac{1-\cos\alpha}{2\sin\alpha} \quad :\alpha \leq \frac{\pi}{2}$ $\frac{1-\cos\alpha}{2} \quad :\frac{\pi}{2} \leq \alpha$	maximum difference of 2% for $\epsilon > 0.13$	4.6%

[1] $\beta = b/a$

between 0.8485 and 0.8491; therefore; it remains approximately constant with an average value of 0.849

$$\frac{k\sqrt{A}\bar{R}}{k\sqrt{A}R_0} = \frac{\bar{R}}{R_0} \cong 0.849. \tag{17}$$

Yovanovich *et al.* [16], [17] already established this result for some specific shapes; the analysis presented here shows that in fact this is generally valid for a wide range of geometries. The nondimensional spreading resistance based on the average temperature for elliptical and rectangular sources is shown in Fig. 16. The predicted resistances are indeed very close. Since the ellipse and rectangle are the lower and the upper bounds for the hyperellipse within $2 \leq n \leq \infty$, it can be concluded that the elliptical source result for nondimensional spreading resistance based on the average temperature can be used for hyperelliptical source within $2 \leq n \leq \infty$. Also, (17) provides an excellent estimate of the ratio $\bar{R}/R_0$.

Since the model provides a good estimate for centroidal temperature based spreading resistance, and (17) is approximately valid for hyperelliptical shapes covering a wide variety of geometries, (17) can be used with confidence to predict the ratio of spreading resistance based on the average and centroid temperatures for a broad variety of heat source shapes. Thus, combining (6) and (17), the model for the average temperature

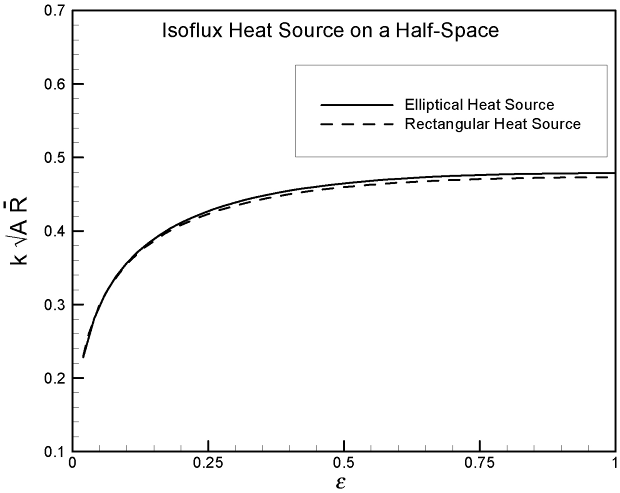

Fig. 16. Comparison of average temperature based spreading resistances for elliptical and rectangular heat sources.

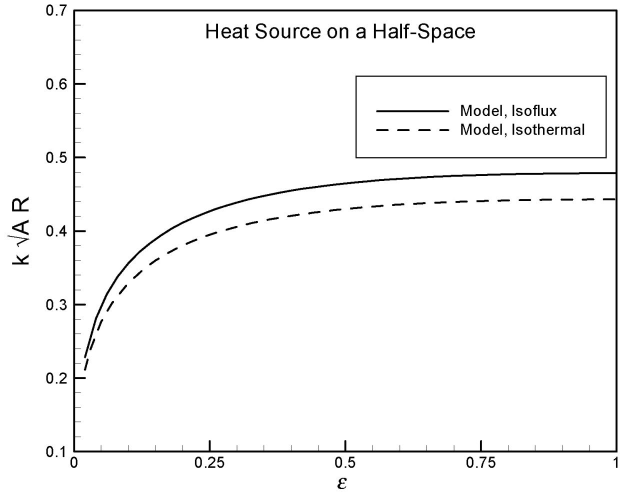

Fig. 17. Proposed model for isothermal and isoflux boundary conditions.

based spreading resistance reads

$$k\sqrt{A}\bar{R} = \frac{1.6974}{\pi\sqrt{\pi}} \frac{K(1-\frac{1}{\epsilon^2})}{\sqrt{\epsilon}}. \tag{18}$$

VII. Boundary Condition

We have so far considered spreading resistance for any isoflux arbitrary-shape heat source on a half-space. Yovanovich [18] developed an analytical solution for an isothermal elliptical source

$$k\sqrt{A}R_T = \frac{\sqrt{\epsilon}}{2\sqrt{\pi}} K(1-\epsilon^2). \tag{19}$$

Schneider [20] numerically solved Laplace's equation for the rectangular source and reported a correlation if the form of

$$k\sqrt{A}R_T = \frac{1}{\sqrt{\epsilon}}\left[0.06588 - \frac{0.00232}{\epsilon} + \frac{0.6786}{(1/\epsilon)+0.8145}\right] \quad : 0.25 \le \epsilon \le 1. \tag{20}$$

A comparison between the solutions of isothermal rectangular and elliptical sources indicates a maximum difference of 1.27% which occurs at $\epsilon = 1$, while the solutions are essentially identical for an aspect ratio ϵ less than 0.4. Since the isoflux elliptical source which is proposed as the model predicts accurately spreading resistance of any isoflux arbitrary-shape heat source, this suggests that the solution for isothermal elliptical source can be used for a wide variety of isothermal heat sources. Thus, the general form of the model for any arbitrary-shape heat source on a half-space can be expressed as

$$k\sqrt{A}R = \begin{cases} \dfrac{1.6974}{\pi\sqrt{\pi}} \dfrac{K(1-\frac{1}{\epsilon^2})}{\sqrt{\epsilon}}, & \text{isoflux (average temp.)} \\ \frac{\sqrt{\epsilon}}{2\sqrt{\pi}} K(1-\epsilon^2), & \text{isothermal.} \end{cases} \tag{21}$$

Fig. 17 presents the spreading resistance for isothermal and isoflux boundary conditions calculated using (21). The ratio of isothermal to isoflux spreading resistance does not change much and remains approximately constant at 0.925 with $R_{\text{isothermal}}/R_{\text{isoflux}} \approxeq 0.925 \pm 0.0005$. In practice, the boundary condition is a combination of isoflux and isothermal conditions and these provide two bounds for actual thermal spreading resistances.

VIII. Summary And Conclusion

Thermal spreading resistance is an important major phenomenon in thermal engineering problems, whenever temperature and cross-sectional area variations exist. In this paper, a model based on the generalization of the analytical solution of isoflux elliptical source has been proposed, and analytic solutions were obtained for a variety of complex shapes. The generalized model presented here provides a unified approach for calculating the spreading resistance for a large variety of geometries, and under both isoflux and isothermal conditions. The highlights of the model and results are as follows.

1) The most appropriate characteristic length scale for nondimensional spreading resistance is square root of area $\sqrt{A}$.
2) The spreading resistance for arbitrarily singly connected shapes agrees with the proposed model.
3) The ratio of isothermal to isoflux spreading resistance is approximately 0.931 for a wide range of shapes for different aspect ratios.

Appendix

Isosceles Trapezoidal Source

The spreading resistance for an isosceles trapezoidal source is found using superposition technique. Considering the parameters shown in Fig. 18, the nondimensional spreading resistance based on the centroidal temperature is found as

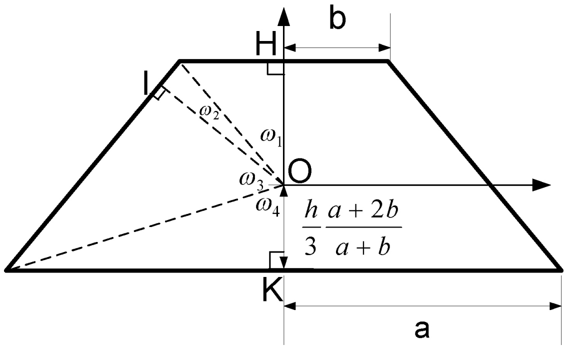

Fig. 18. Cross-section of an isosceles trapezoidal heat source.

$$k\sqrt{A}R_0 = \frac{1}{\pi}\frac{\overline{OI}\,(\Omega_2+\Omega_3)+\overline{OH}\Omega_1+\overline{OK}\Omega_4}{\sqrt{A}} \qquad (22)$$

where $\Omega_i = \ln[\tan((\pi/4)+(\omega_i/2))]$. For $\theta > 90$, Ω_2 and ω_2 must be replaced by $-\Omega_2$ and $-\omega_2$, respectively.

REFERENCES

[1] J. A. Greenwood and B. P. Williamson, "Contact of nominally flat surfaces," *Proc. R. Soc. Lond. Ser. A, Math. Phys. Sci.*, vol. 295, pp. 300–319, Dec. 1966.

[2] D. Tabor, *The Hardness of Metals*. London, U.K.: Oxford Univ. Press, 1951, ch. 1.

[3] A. K. Das and S. S. Sadhal, "Thermal constriction resistance between two solids for random distribution of contacts," *Heat Mass Transfer*, vol. 35, no. 2, pp. 101–111, Jul. 1999.

[4] A. A. Rostami, A. Y. Hassan, and P. C. Lim, "Parametric study of thermal constriction resistance," *Heat Mass Transfer*, vol. 37, no. 1, pp. 5–10, Jan. 2001.

[5] Y. Muzychka, M. Yovanovich, and J. Culham, "Application of thermal spreading resistance in compound and orthotropic systems," in *Proc. Am. Inst. Aeronaut. Astronaut. (AIAA) 39th Aerospace Sci. Meeting Exhibit*, Reno, NV, Jan. 2001, p. 0366.

[6] D. P. Kennedy, "Spreading resistance in cylindrical semiconductor devices," *J. Appl. Phys.*, vol. 31, pp. 1490–1497, Aug. 1960.

[7] M. M. Yovanovich, "Four decades of research on thermal contact, gap, and joint resistance in microelectronics," *IEEE Trans. Compon. Packag. Technol.*, vol. 28, no. 2, pp. 182–206, Jun. 2005.

[8] A. M. Clausing and B. T. Chao, "Thermal contact resistance in a vacuum environment," *J. Heat Transfer Trans. ASME*, vol. 87, no. 2, pp. 243–251, 1965.

[9] B. B. Mikic, "Thermal contact conductance; Theoretical considerations," *Int. J. Heat Mass Transfer*, vol. 17, no. 2, pp. 205–214, 1974.

[10] M. G. Cooper, B. B. Mikic, and M. M. Yovanovich, "Thermal contact conductance," *Int. J. Heat Mass Transfer*, vol. 12, pp. 279–300, Jan. 1969.

[11] Y. S. Muzychka, M. M. Yovanovich, and J. R. Culham, "Thermal spreading resistance of eccentric heat sources on rectangular flux channels," *ASME J. Electron. Packag.*, vol. 125, no. 2, pp. 178–185, 2003.

[12] G. N. Ellison, "Maximum thermal spreading resistance for rectangular sources and plates with nonunity aspect ratios," *IEEE Trans. Compon. Packag. Technol.*, vol. 26, no. 2, pp. 439–454, Jun. 2003.

[13] S. Karmalkar, P. V. Mohan, H. P. Nair, and R. Yeluri, "Compact models of spreading resistances for electrical/thermal design of devices and ICs," *IEEE Trans. Electr. Devices*, vol. 54, no. 7, pp. 1734–1743, Jul. 2007.

[14] M. Pawlik, "Spreading resistance: A quantitative tool for process control and development," *Vacuum Sci. Technol. B: Microelectr. Nanometer Struct.*, vol. 10, pp. 388–396, Jan. 1992.

[15] M. M. Yovanovich, "Thermal constriction resistance of contacts on a half-space: Integral formulation," *Progress Astronaut. Aeronaut.: Radiative Transfer Thermal Control*, vol. 49, pp. 397–418, 1976.

[16] M. M. Yovanovich, S. S. Burde, and J. C. Thompson, "Thermal constriction resistance of arbitrary planar contacts with constant flux," *Progress Astronaut. Aeronaut.: Thermophys. Spacecraft Outer Planet Entry Probes*, vol. 56, pp. 127–139, 1976.

[17] M. M. Yovanovich and S. S. Burde, "Centroidal and area average resistances of nonsymmetric, singly connected contacts," *AIAA J.*, vol. 15, pp. 1523–1525, Oct. 1977.

[18] M. M. Yovanovich, "Thermal constriction resistance between contacting metallic paraboloids: Application to instrument bearings," *Progress Astronaut. Aeronaut.: Fundam. Spacecraft Thermal Design*, vol. 24, pp. 337–358, 1971.

[19] H. S. Carslaw and J. C. Jaeger, *Conduction of Heat in Solids*, 2nd ed. London, U.K.: Oxford Univ. Press, 1959, ch. 3.

[20] G. E. Schneider, "Thermal resistance due to arbitrary dirichlet contacts on a half-space," *Prog. Astronaut. Aeronaut. Thermophys. Therm. Control*, vol. 65, pp. 103–119, 1978.

Ehsan Sadeghi received the B.A.Sc. and M.A.Sc. degrees in mechanical engineering from Sharif University of Technology, Tehran, Iran. He is currently working toward the Ph.D. degree from the Department of Mechanical Engineering, University of Victoria, Victoria, BC, Canada. For the Ph.D. degree, he has been working on the analytical and experimental investigations of transport phenomena in high porosity materials including metal foams, and gas diffusion layers used in fuel cells.

His other research interests include contact mechanics, renewable energy, microscale heat transfer, microfluidics, and microelectronics cooling.

Mr. Sadeghi is a Member of the Institute for Integrated Energy Systems and the Multiscale Thermofluidic Laboratory for Sustainable Energy Research.

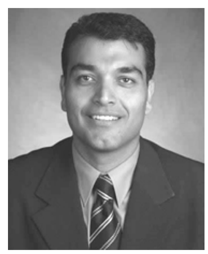

Majid Bahrami received the B.A.Sc. degree in mechanical engineering from Sharif University of Technology, Tehran, Iran, in 1992, the M.A.Sc. degree in gas-solid flow in circulating fluidized beds from Amir Kabir University of Technology (Tehran Polytechnic), Tehran, Iran, in 1995, and the Ph.D. degree in thermal joint resistance of contacting rough surfaces from the Department of Mechanical Engineering, University of Waterloo, Ontario, Canada, in 2004.

From 1995 to 2000, he practiced in heating, ventilating, air conditioning, and refrigeration industry as a Thermal Engineer and Consultant. From 2004 to 2006, he was a Post-Doctoral Fellow and an Instructor with the Microelectronics Heat Transfer Laboratory, Waterloo, Ontario, Canada, where he made major contributions in the field of heat transfer, microfluidics, and microelectronics cooling. From 2006 to 2008, he was an Assistant Professor with the Department of Mechanical Engineering, University of Victoria, Victoria, BC, Canada. Since 2008, he has been an Assistant Professor with the School of Engineering, Simon Fraser University, BC, Canada. He has numerous publications in refereed journals and conferences. His current research interests include modeling and characterization of transport phenomena in micro/nano-structured materials and porous media, heat transfer in microchannels and microfluidics, conversion and storage of sustainable energy, contact mechanics and thermal interfaces, and microelectronics cooling.

He is a Member of the American Society of Mechanical Engineers, the American Institute of Aeronautics and Astronautics, and the Canadian Society for Mechanical Engineering.

Ned Djilali received a B.S. (Hons.) in aeronautical engineering from the University of Hertfordshire, Herts, U.K., the M.S. degree in aeronautics and fluid mechanics from Imperial College, London, U.K., and the Ph.D. degree in mechanical engineering from the University of British Columbia, Vancouver, BC, Canada.

He is the Canada Research Chair in Energy Systems Design and Computational Modeling and a Professor of Mechanical Engineering with the Department of Mechanical Engineering, University of Victoria, Victoria, BC, Canada. He has served as the Director of the Institute for Integrated Energy Systems from 2001 to 2007, promoting interdisciplinary research across science and technology, economics and policy. Prior to joining the University of Victoria in 1991, he was an Aerodynamicist with the

Canadair Aerospace Division, Bombardier, Inc., Montreal, from 1989 to 1991. He has published over 100 peer reviewed journal papers, and holds several patents and research awards. His current research and teaching interests include transport phenomena and sustainable energy systems, with a focus on fuel cell technology, hydrogen systems safety, and integration of renewable energy. Much of his research is in collaboration with leading fuel cell companies in North America and Japan.

Dr. Djilali is a Fellow of the Canadian Academy of Engineering.